WATERLINE DETECTION AND MONITORING IN THE GERMAN WADDEN SEA USING HIGH RESOLUTION SATELLITE-BASED RADAR MEASUREMENTS

S. Wiehle[a, ∗], S. Lehner[a], A. Pleskachevsky[a]

[a] DLR, Maritime Security Lab, 28201 Bremen, Germany - (stefan.wiehle, susanne.lehner, andrey.pleskachevsky)@dlr.de

KEY WORDS: North Sea, Wadden Sea, bathymetry, coastal processes, remote sensing, radar satellites

ABSTRACT:

High resolution TerraSAR-X/TanDEM-X as well as Sentinel-1 remote sensing Synthetic Aperture Radar (SAR) data are used to determine and monitor the waterline in the Wadden Sea. In this very unique and dynamic coastal region in the southeastern North Sea, tidal flats extend several kilometers away from the coast during low tide with features like tidal inlets and sand banks. Under the influence of tidal water currents transporting large amounts of eroded material, inlets and sand banks move over time; heavy storms can even cause large variations in their extensions in merely a few hours. Observation of these obstacles is crucial for maritime security as high ship traffic is caused by the ports of Hamburg, Bremerhaven, Wilhelmshaven and others. Conventional monitoring campaigns with ships or airplanes are economically expensive and can only provide limited coverage. We present an automatic algorithm with Near Real-Time capability for extracting the waterline at the time of recording from SAR images, which allows for a fast and large scale determination of changes in coastal outlines. The comparison of recent acquisitions of TerraSAR-X and Sentinel-1 to bathymetry data of the Elbe estuary obtained in 2010 reveals significant changes in tidal flat structures.

1. INTRODUCTION

At the coast of the southeastern North Sea, a strip of up to $20\,\mathrm{km}$ of land falls dry twice daily, forming the Wadden Sea. During low tide, features like tidal flats, tidal inlets and sand banks appear. Under the influence of tidal currents, these structures are eroded with erosion rates of up to several meters per month. This is even more accelerated in case of heavy storms and storm surges, where a single event can cause the same changes as several months of fair-weather conditions (Herrling and Winter, 2014). Besides these unique and protected natural landscape, the Wadden Sea is also an area of high ship traffic to the largest German ports of Hamburg, Bremerhaven, Wilhemshaven and others. Hence, monitoring topographic changes in the Wadden Sea like the positions of sand banks is essential for maritime safety. Due to the large area, conventional monitoring campaigns with ships or airplanes are economically expensive while providing only limited coverage. With Synthetic Aperture Radar (SAR) satellites like TerraSAR-X/Tandem-X and Sentinel-1, frequent monitoring of large areas is possible with resolutions of 1 to 10 meters.

We present an algorithm that automatically detects the waterline in a single-polarization SAR scene, where special emphasis was put to Wadden Sea scenes. Regular coasts consisting of dry sand, grass or cliffs will usually yield a Normalized Radar CrossSection (NRCS) σ_0 clearly above the sea water and have only few small-scale structures like tidal inlets. Tidal mudflats, on the other hand, consist of a mix of highly reflective dry sand, mud and shallow water puddles acting as a specular reflector yielding almost no reflectivity. Hence, the NRCS of these surfaces strongly varies from very high levels to very low levels (van der Wal et al., 2005). The NRCS of the surrounding seawater is determined by wind field conditions (Li and Lehner, 2014) and often higher than mudflat areas. As a consequence, algorithms using scene brightness as primary criterion (e.g. Acar et al., 2012; Liu and Jezek, 2004) will work well in high tide, but are hardly applicable to low tide Wadden Sea scenes. Algorithms like Dellepiane et al. (2004); Yu and Acton (2004); Gade et al. (2014) use interferometric, polarimetric or multi-band SAR data; however, we
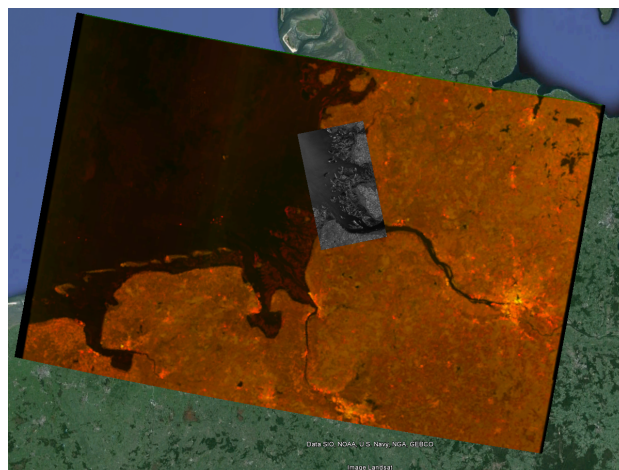

Figure 1: Comparison of the Sentinel-1 Interferometric Wide Swath scene and the TerraSAR-X stripmap scene over the North Sea coast. *Background image ©Google Earth.*

focus on frequently acquired single-polarized, non-polarimetric scenes aiming for wide applicability. The presented algorithm is intended to work in Near Real-Time (NRT) processing chains; hence, automatic operation with short runtime is a requirement.

We use data from the TerraSAR-X/TanDEM-X (X-band) and from Sentinel-1 (C-band) satellites. TerraSAR-X (TS-X) and TanDEM-X were launched in 2007 and 2010, respectively. The altitude of their sun-synchronous orbit is $514\,\mathrm{km}$. Their resolution in stripmap (SM) mode is $3 \times 3\,\mathrm{m}$ with a swath width of $30\,\mathrm{km}$. For our purpose, this stripmap mode provides a good compromise between resolution and coverage. Sentinel-1A (S1A), the first satellite of the Sentinel earth observation program, was launched in 2014 with an orbit altitude of $693\,\mathrm{km}$. The mode with highest resolution currently available for the Wadden Sea region is the Interferometric Wide Swath (IW) mode, which has a resolution of $5 \times 20\,\mathrm{m}$ and a swath width of $250\,\mathrm{km}$. An overview of the two scenes used here is shown in Fig. 1. Table 1 provides details of both acquisitions.
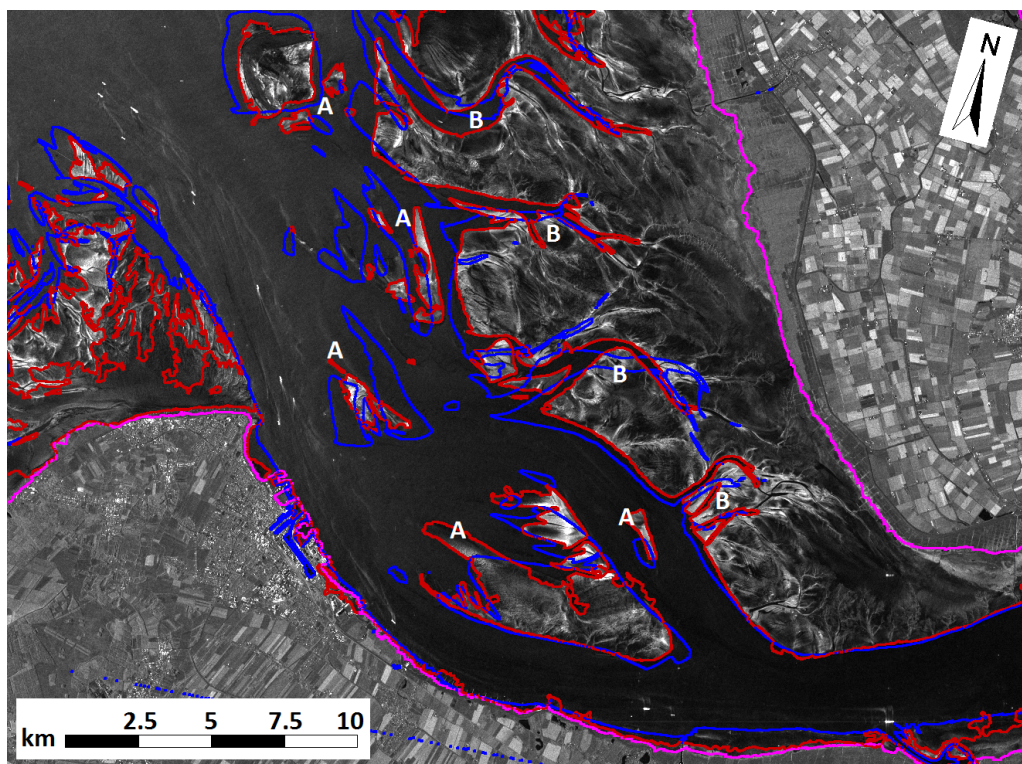

∗Corresponding author

Figure 2: Sub-scene of a TerraSAR-X SM scene of the Elbe estuary, acquisition parameters are given in Table 1. The red lines indicate the boundaries found by our algorithm, the blue lines indicate the Lowest Astronomical Tide (LAT) level according to the bathymetry data and the magenta lines show the SWBD coastline. The letters indicate selected differences to the bathymetry data for shifted sand banks (A) and tidal inlets (B).

2. DESCRIPTION OF THE ALGORITHM

The goal of our algorithm is to create, from a SAR acquisition, a binary landmask indicating land and water which can be used for later analysis. The algorithm is divided into a preparation phase, an iteration phase and a finalization phase.

2.1 Preparation phase

In the beginning, the algorithm performs the following steps:

- Rescaling and sub-scene selection
  As high resolution SAR scenes correspond to very large image sizes, the scene is resized by a scaling factor S. Furthermore, a sub-scene of the image can be chosen to limit all further processing to the respective area. This step is only necessary to reduce runtime and similarly also used in other value-adding maritime SAR products. If runtime is not a concern and full resolution processing of the entire scene is to be performed, this entire step can be omitted.

- Logarithmic scaling
  In preparation for the upcoming edge detection, the input image is converted to logarithmic scale. Edge strength, which is determined by contrast, is thereby increased in dark areas like water and mudflats. It is decreased in bright areas like mainland structures, however, these are not important for waterline detection.

- Median smoothing
  The scene is smoothed twice using a median filter, which reduces high frequency edges due to speckle while preserving relevant image edges. The size of the smoothing window should be small enough to not remove small structures

like tidal creeks, but must be large enough to sufficiently reduce speckle for the edge detection. We achieved good and consistent results using a smoothing window size of $2n + 1 \times 2n + 1$, where $n = 8/S$; hence, larger windows are used for lower scaling factors.

- Edge detection
  Edge detection using the Sobel operator is performed on the smoothed image, resulting in an image containing thick edges of varying intensity. This image is used in each iteration during the next phase.

- Brightness landmask
  A binary landmask is generated from the smoothed image, hereafter referred to as brightness landmask. The threshold is defined using Otsus method for automatic gray-level thresholding (Otsu, 1979). In most scenes of the Wadden Sea showing mainland and strongly reflecting tidal structures, this thresholding works quite well and is used as comparison during the iteration phase. Dark mudflats, on the other hand, will be marked as sea in this landmask; hence, it is not suitable as the only landmasking method for tidal flat areas.

- SWBD landmask
  Another binary landmask is generated from data of the Shuttle Radar Topography Mission (SRTM) Water Body Data (SWBD), which we will call SWBD landmask hereafter. The SWBD landmask provides the starting points for the flood fill algorithm in the iteration phase. In case the SWBD coastline is not available for the respective scene, this step can be omitted and the brightness landmask is used instead, which is more prone to error due to possible high reflectivity of near range sea water or low reflectivity of land structures or inner lakes.
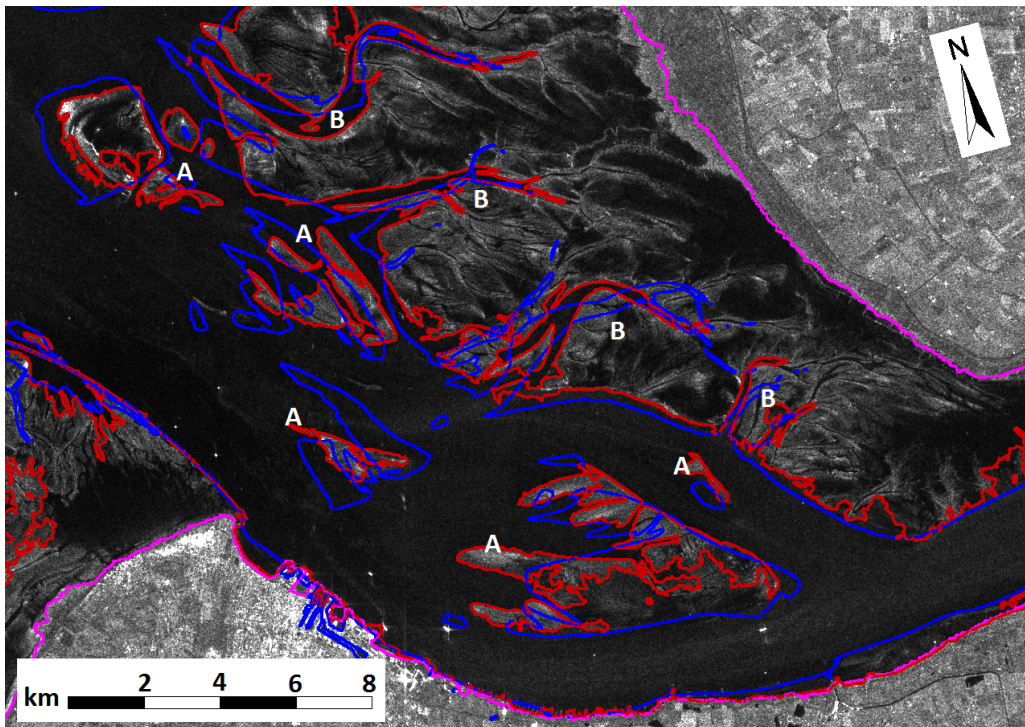
Figure 3: Sub-scene of a Sentinel-1 IW scene of the Elbe estuary, acquisition parameters are given in Table 1. The red lines indicate the boundaries found by our algorithm, the blue lines indicate the Lowest Astronomical Tide (LAT) level according to the bathymetry data and the magenta lines show the SWBD coastline. The letters indicate selected differences to the bathymetry data for shifted sand banks (A) and tidal inlets (B).

2.2 Iteration phase

In the second part of the algorithm's work flow, the following steps are repeated to generate a preliminary binary landmask:

- Edge drawing
  The image previously created by the edge detection step contains thick edges of varying intensity, which are now turned into thin binary edges. The edge drawing technique (Topal and Akinlar, 2012) is an alternative approach to edge thinning: It is redrawing lines starting from strong edge points (anchor points) determined by an upper threshold T_u, then running along pixels of highest relative edge strength whereby a lower threshold T_l determines the noise level, i.e. edges which are not followed.

- Gap closing
  While the edge drawing method generally creates closed contours as long as the underlying edges are sufficiently strong, we found that regions of land-water edges below the noise level are quite common. As no gaps may be present between water and land for the following flood fill algorithm, this routine attempts to close missing links. Starting from a dead-end edge point, a cone around the previous edge direction is scanned, the closest edge point found within a specified radius is connected in a straight line.

- Flood filling
  The image with thin and closed binary edges is now transformed to a binary landmask using a flood fill procedure. The starting points are chosen from the corners of the scene if the SWBD landmask suggests water at the respective point. The flood filling extends to all pixels in a 4-neighborhood that are no edges and marks them as water, resulting in a binary landmask which we will refer to as flood fill landmask.

- Landmask comparison
  The flood fill landmask is now compared to the brightness landmask; each equal pixel value adds a point to a final agreement score. There will almost never be a perfect agreement as the flood fill landmask does not contain inner lakes and the brightness based landmask does not contain dark mud flats. Nevertheless, if large areas of the land are flooded due to too high thresholds or if many parts of the sea are shown as land because of too low thresholds, the resulting score will be low.

While a landmask is already generated after the first flood filling step, its validity is strongly dependent on the thresholds T_u and T_l used during the edge drawing. As the algorithm is supposed to run without user interaction and appropriate threshold levels were found to vary from scene to scene depending on acquisition conditions, a method to automatically set the thresholds is needed. We use a hill climbing method for finding the optimal agreement value: the environment of the current threshold pair $(T_u \pm \Delta T_u, T_l \pm \Delta T_l)$ is investigated using the four steps described above with the respective thresholds. If a higher agreement value is found, the procedure is repeated with the corresponding thresholds set as current value. The iteration ends when no higher agreement value is found in the neighborhood of the current value; depending on the scene, this usually requires a number of 10-30 investigated threshold pairs.

2.3 Finalization phase

Two more steps are performed on the landmask resulting from the iteration phase:

- Region testing
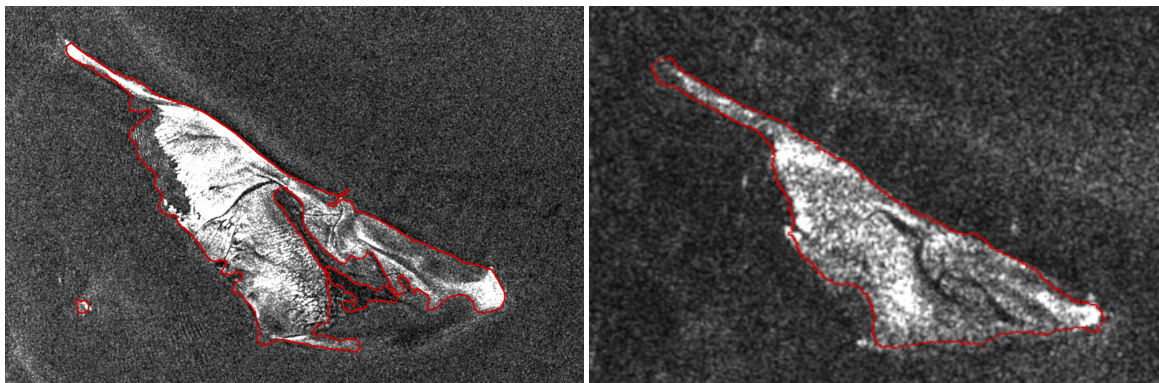 Land regions adjacent to water are tested to determine if the

Figure 4: Full resolution comparison of the TerraSAR-X SM scene (left, 2.75 m pixel spacing) and the Sentinel-1 IW scene (right, 10 m pixel spacing). The red lines indicate the boundaries found by our algorithm.

Scene	Band	Mode	Pol.	Pixel spacing	Acquisition Date UTC	Cuxhaven Water Level	Wind speed U_{10}
TerraSAR-X	X	SM	VV	2.75 m × 2.75 m	2014-11-19 17:02	369 cm	5.5 m/s
Sentinel-1	C	IW	VV	10 m × 10 m	2015-01-19 05:41	343 cm	2.5 m/s

Table 1: Acquisition parameters for the presented scenes. The TS-X scene was acquired in stripmap (SM) mode while the Interferometric Wide Swath (IW) mode was used for the Sentinel-1 scene.

separating edge does really separate water from land. For every point on the border between land and see, the average brightness of the adjacent sea pixels is compared against the average brightness of the respective land region. The land region is hereby limited by the edges taken from the binary edge image while brightness levels are taken from the smoothed gray-level image. If brightness and variance are similar, the apparent land region is set to water in the landmask. This step strongly increases the reliability of the landmask by removing regions created by water structures like false islands and peninsulas.

- Small islands removal
  Very small landmasses surrounded by sea are set to water. This reduces errors due to ships and buoys which are not removed during the region testing step because of their high brightness levels.

The landmask received after these steps is the output of the algorithm.

3. RESULTS

We present the results of our algorithm for the Elbe estuary near Cuxhaven, Germany. We show the results for a TS-X and a Sentinel-1 acquisition in Fig. 2 and 3, respectively; the acquisition details are given in Table 1. For comparison, we have included in the scenes the topography obtained by the German Federal Waterways Engineering and Research Institute (BAW) in 2010 with 5×5 m resolution; the blue lines show the Lowest Astronomical Tide (LAT) level for Cuxhaven. The magenta lines in the figures show the SWBD coastlines recorded in 2000 which is provided in 1 arcsec (≈ 30 m) resolution. The results of our algorithm are shown with red lines. Both scenes were recorded around $20 - 30$ minutes after low tide, showing a large amount of exposed tidal flats. These tidal flat areas appear similar in X- and C-band, which is in accordance to the observations of Gade et al. (2014).

In both scenes, comparing the BAW topography to the SAR data reveals the significant changes of the tidal flats during the last 5 years. Sand banks in the Elbe have apparently shifted position and/or extension as many highly reflective bright parts can

be seen in areas lower than LAT level according to the topography; we have marked five such occurrences with A in Figs. 2 and 3. The position of many tidal inlets also has changed, in some cases by more than 150 m, which is easily visible in the tidal flats west of the Elbe; we marked four such areas with the letter B.

The SWBD coastline is shown in both figures also for comparison. While it is still accurate in the Cuxhaven harbor areas and the southern part of the Elbe fairway, it does not cover the tidal flats. In the Wadden Sea, an application for landmasking, needed for the generation of several value-added SAR products, is only possible during high tide without tidal flats.

In both presented scenes our algorithm successfully tracks most of the waterline structures. The identified waterlines are usually on the same pixel compared to manual determination, which is achieved by their construction using only little smoothing and the edge drawing approach following the pixels of highest gradient strength. This combination also allows the tracking of tidal inlets up to a width of the smoothing window; thinner inlets are removed by the smoothing.

Our algorithm encounters challenges when the contrast is weak in some areas of a single waterline and the edge is interrupted. This leads to the flooding and non-detection of areas with large contrast. Although the gap closing step significantly improves the algorithm's reliability in such cases, it currently does not identify all cases where closing gaps would be necessary.

Figure 4 shows the scenes from Figs. 2 and 3 in their respective full (pixel) resolution (2.75 m for TS-X SM and 10 m for S1 IW). Due to the higher resolution, the TS-X SM mode shows much more details while Sentinel-1 IW mode, as shown in Fig. 1, has a much larger coverage. A comparison of the sandbank extensions shows that the southern part is apparently flooded during the TS-X acquisition, but has fallen dry during the time of the S1A acquisition, which is possible considering the difference in water level given in Table 1.

The goal to have the runtime of our algorithm fulfill NRT requirements is achieved. The processing time of full TS-X stripmap scene with a scaling factor of 4 (resulting in ≈ 15 MPx) is around 3 min on our notebook PC equipped with an Intel(R)Core(TM)2 Extreme Q9300 CPU running at 2.53 GHz. Lower scaling factors

may require faster hardware generally available on NRT processing stations.

4. SUMMARY AND OUTLOOK

We developed an algorithm for automatic waterline detection from SAR images with focus on the Wadden Sea. The algorithm first performs scaling, smoothing and edge detection, followed by iterated edge drawing and flood filling to determine an optimal agreement value by comparing to a brightness landmask. The final steps consist of region testing and small islands removal. The binary landmask generated as output can be used for further processing steps, like monitoring of the tidal topography combining several acquisitions at different tidal states. It can also be used for further maritime SAR products which require landmasking, like ship detection or wind and wave processing.

By comparing SAR data from 2014/2015 with bathymetry data from 2010, the strong changes in the investigated area became very obvious. The algorithm was able to detect the mainland and many tidal flat areas in the scenes shown, the determined water lines generally align with the boundaries determined by eye. Due to its short runtime of only a few minutes, it is also well-suited for use in Near Real Time (NRT) processing chains. Some parts may remain undetected due to remaining gaps in the edges where the current implementation of gap closing does not work; this will be improved in future versions of the algorithm.

With Sentinel-1A already in operation and its twin Sentinel-1B set to launch in early 2016, tidal flats will be regularly seen on their SAR data of the southeastern North Sea coasts. With this large amount of available data, automatic algorithms will be of great importance for frequent waterline monitoring, allowing to track the morphology of tidal flat structures. Niedermeier et al. (2005) and Heygster et al. (2010) demonstrated that also the topography can be determined from the waterline data by combining acquisitions of several tidal states and water level data. These monitoring tasks can be carried out with Sentinel-1 data using automatic waterline detection processors and supported by high-resolution TS-X products for times of strong changes or areas with small scale structures.

ACKNOWLEDGEMENTS

References

Acar, U., Bayram, B., Sanli, F. B., Abdikan, S., Sunar, F. and Cetin, H. I., 2012. An Algorithm for Coastline Detection Using SAR Images. Int Arch Photogram Rem Sens Spatial Inform Sci pp. 457–460.

Dellepiane, S., De Laurentiis, R. and Giordano, F., 2004. Coastline extraction from SAR images and a method for the evaluation of the coastline precision. Pattern Recogn. Lett. 25(13), pp. 1461–1470.

Gade, M., Melchionna, S., Stelzer, K. and Kohlus, J., 2014. Multi-frequency SAR data help improving the monitoring of intertidal flats on the German North Sea coast. Estuar. Coast. Shelf. S. 140(0), pp. 32–42.

Herrling, G. and Winter, C., 2014. Morphological and sedimentological response of a mixed-energy barrier island tidal inlet to storm and fair-weather conditions. Earth Surf. Dyn. 2(1), pp. 363–382.

Heygster, G., Dannenberg, J. and Notholt, J., 2010. Topographic mapping of the German tidal flats analyzing SAR images with the waterline method. IEEE T. Geosci. Remote 48, pp. 1019–1030.

Li, X.-M. and Lehner, S., 2014. Algorithm for Sea Surface Wind Retrieval From TerraSAR-X and TanDEM-X Data. IEEE T. Geosci. Remote 52, pp. 2928–2939.

Liu, H. and Jezek, K. C., 2004. Automated extraction of coastline from satellite imagery by integrating Canny edge detection and locally adaptive thresholding methods. Int. J. Remote Sens. 25, pp. 937–958.

Niedermeier, A., Hoja, D. and Lehner, S., 2005. Topography and morphodynamics in the German Bight using SAR and optical remote sensing data. Ocean Dynam. 55, pp. 100–109.

Otsu, N., 1979. A threshold selection method from gray-level histograms. IEEE T. Syst. Mam Cyb. 9(1), pp. 62–66.

Topal, C. and Akinlar, C., 2012. Edge drawing: A combined real-time edge and segment detector. J. Vis. Commun. Image R. 23(6), pp. 862–872.

van der Wal, D., Herman, P. and Wielemaker-van den Dool, A., 2005. Characterisation of surface roughness and sediment texture of intertidal flats using ERS SAR imagery. Remote Sens. Environ. 98(1), pp. 96–109.

Yu, Y. and Acton, S. T., 2004. Automated delineation of coastline from polarimetric SAR imagery. Int. J. Remote Sens. 25(17), pp. 3423–3438.